A Methanol-Tolerant Gas-Venting Microchannel for a Microdirect Methanol Fuel Cell

Dennis Desheng Meng, *Member, IEEE*, Thomas Cubaud, Chih-Ming Ho, *Member, IEEE*, and Chang-Jin Kim, *Member, IEEE*

***Abstract*—As a byproduct, CO_2 gas is constantly generated from the electrochemical reactions of direct methanol fuel cells (DMFCs). In the anodic channel of a DMFC, the gas forms bubbles, which leads to bubble clogging and pressure buildup if the device is miniaturized. Bubble clogging increases the flow resistance in microchannels, calling for excessive power consumption for fuel delivery. Pressure buildup aggravates the undesired crossover of methanol. In order to solve those problems, this paper introduces a gas-venting microchannel that directly removes gas bubbles from the two-phase flows of gas and methanol solution without leakage. By employing a hydrophobic nanoporous membrane, successful venting is achieved for both water and methanol fuel with a concentration of as high as 10 M. The fuel is contained without leakage under overpressures of as high as 200 kPa for both water and 10-M methanol, fulfilling the requirement of the current- as well as next-generation microdirect methanol fuel cells. A 1-D venting rate model is developed and experimentally verified for elongated bubbles. The reported bubble removal approach is also useful for other microfluidic devices, in which the accidental introduction of gas bubbles is prevalent. [2006-0001]**

***Index Terms*—Fuel cells, microfluidics, surface tension, two-phase flow.**

I. Introduction

GAS bubbles present a major challenge for modern microfluidic devices, including microfuel cell systems and micrototal analysis systems. Gas bubbles in a liquid-filled microchannel are known to increase the flow resistance and even block the flow [1], [2], becoming a significant burden on the robust design. If the microfluidic device is sealed, the generation of gas bubbles increases the internal pressure and may even damage the device. Aside from pressure considerations, gas bubbles can block the reactant from the surfaces of the catalyst, electrodes, or sensing components, negating the inherent benefit of microreactors (i.e., high area-to-volume ratios). It has been widely realized that the accidental introduction of gas bubbles is prevalent in microfluidic devices, which is often caused by the priming process or fluctuations in pressure or temperature. Although "bypass" [3], "trapping" [4], and specifically shaped microchannels [5] have been proposed to relieve the bubble clogging problem, these solutions retain the undesired gas within the system and can only tolerate a limited amount of gas.

If a large volume of gas is generated over time, the gas bubbles should be promptly removed. This is the situation of microfuel cells with organic liquid fuel (e.g., methanol, formic acid, and glucose), in which gas bubbles are continuously generated inside the microchannel as a result of the chemical reaction. Although the issue is common to most types of fuel cells with organic liquid fuel, we use the direct methanol fuel cell (DMFC) as a specific example in this paper because of its current acceptance as the power source for next-generation consumer electronics [6]. The working principle of a DMFC is illustrated in Fig. 1. The methanol aqueous solution is fed into the anodic channel while air flows through the cathodic channel. A series of electrochemical reactions is enabled by the membrane electrode assembly (MEA), which includes the proton exchange membrane (PEM), electrodes, and catalyst layers. Protons migrate from the anodic side to the cathodic side through the PEM, while electrons are collected by the anode and consumed in the cathode. The accumulated electrons provide the continuous current for the external circuit.

In the fuel stack of a DMFC, the electrochemical reactions are

$$\mathrm{CH_3OH + H_2O \rightarrow 6e^- + 6H^+ + CO_2 \uparrow} \quad \text{(anodic side)}$$

$$\mathrm{1.5O_2 + 6e^- + 6H^+ \rightarrow 3H_2O} \quad \text{(cathodic side)}$$

$$\mathrm{CH_3OH + 1.5O_2 \rightarrow 2H_2O + CO_2 \uparrow} \quad \text{(overall reaction).}$$

According to these reactions, DMFCs intrinsically generate CO_2 gas bubbles. In a large-scale stationary DMFC, the generation of these small bubbles may not substantially affect the fuel cell's performance. The gas byproduct is usually carried downstream with the exiting fuel flow to an external gas/liquid separator, which is essentially an open tank, where they are released. However, the CO_2 gas bubbles can cause serious bubble clogging problems in a microdirect methanol fuel cell (μDMFC) [7] since their sizes are comparable to the characteristic dimension of the anodic microchannel. The continuous bubble generation makes the bubble-clogging problem of microfuel cells more severe than most other microfluidic devices. Wong *et al.* [8] have indeed experimentally confirmed

Manuscript received January 31, 2006; revised November 7, 2006. This work was supported by the Defense Advanced Research Projects Agency Micro Power Generation Program. Subject Editor K. Bohringer.

D. D. Meng was with the Department of Mechanical and Aerospace Engineering, University of California, Los Angeles, CA 90095-1597 USA. He is now with the Department of Mechanical Engineering–Engineering Mechanics, Michigan Technological University, Houghton, MI 49931-1295 USA (e-mail: dmeng@mtu.edu).

T. Cubaud was with the Department of Mechanical and Aerospace Engineering, University of California, Los Angeles, CA 90095-1597 USA. He is now with the Department of Mechanical Engineering, Stony Brook University, Stony Brook, NY 11794 USA.

C.-M. Ho and C.-J. Kim are with the Department of Mechanical and Aerospace Engineering, University of California, Los Angeles, CA 90095-1597 USA.

Color versions of one or more of the figures in this paper are available online at http://ieeexplore.ieee.org.

Digital Object Identifier 10.1109/JMEMS.2007.910241

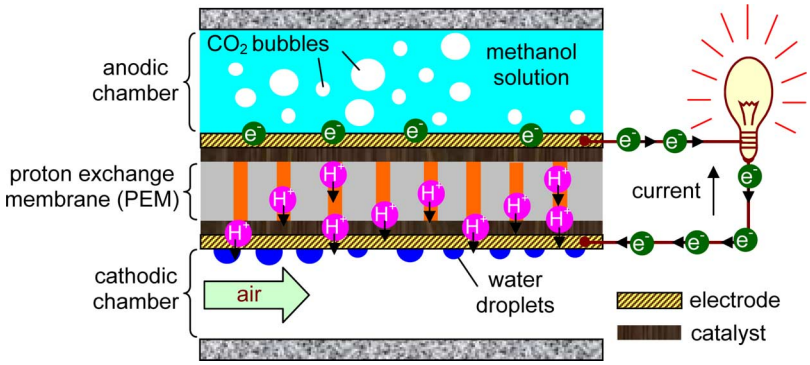

Fig. 1. Working principle of a DMFC.

that CO_2 bubble evolution significantly affects the performance of the μDMFC and have further provided the characterization results. Moreover, gas bubbles cause an additional problem that is critical to the MEA-based fuel cells, such as μDMFC: The elevated pressure in the anodic microchannel can significantly increase the methanol crossover from the anodic side to the cathodic side through the PEM [9], which is detrimental. Therefore, it is most desired to vent these bubbles out directly from the anodic microchannel of a μDMFC as they are generated. However, a simple opening downstream of the anodic microchannel, which is the direct counterpart to the gas separator of a large-scale stationary DMFC, is not an ideal solution. The risk of fuel leakage is unacceptable for μDMFCs, which are usually designed for portable applications, such as laptop computers or cell phones. Meng *et al.* [10], [11] have verified that hydrophobic microscopic capillaries can vent out CO_2 bubbles from water-based liquid without leakage under moderate pressure (less than 3 kPa). Noting that the ability to prevent leakage dramatically increases when the hydrophobic capillaries shrink down to submicrometer diameters, we introduce hydrophobic nanoporous membranes into the device fabrication. In this paper, we report a gas-venting microchannel that can handle organic liquid fuels. A main goal of this paper is to accommodate a methanol aqueous solution even at a high concentration (up to 10 M) to prepare for next-generation fuel cells. In addition to μDMFC, the reported technology in this paper also applies to microbial (glucose) fuel cells [12], portable dialysis devices [13], water recycling systems for space shuttles [14], degassers for high-performance liquid chromatography (HPLC) [15], and micromixers [16], among others.

II. Working Mechanism

The proposed gas removal approach is implemented by microscopic hydrophobic capillaries, which allow the gas to pass through relatively undeterred while the liquid menisci blocks the liquid from flowing out. For the methanol aqueous solution, these capillaries are also nonwetting, with contact angles that are considerably larger than 90°, as shown in Table I. Fig. 2(a) represents an idealized model to illustrate how the liquid can be restricted from leaking by its own meniscus. On the sharp corner of the venting capillary's entrance, this meniscus can assume a range of curvatures, so as to balance

TABLE I
Interfacial Properties of the Methanol Aqueous Solution

		water	1M	2M	10M	100% Methanol
Contact angle on Teflon® flat surface	Advancing	122°	119°	120°	101°	67°
	Receding	105°	102°	99°	60°	60°
	Hysteresis	17°	17°	21°	41°	7°
Surface tension (10^{-3}N/m)		72.8	66.5	57.4	39.7	22.7

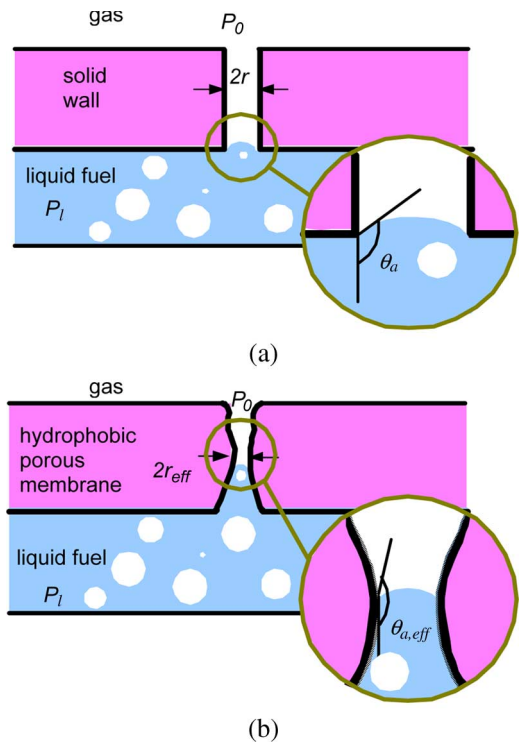

Fig. 2. Small meniscus in a hydrophobic capillary prevents liquid leakage. (a) Idealized straight and smooth capillary. (b) Realistic capillary of irregular shape.

with the varying pressures across the meniscus (transmeniscus pressure) according to the Laplace–Young equation given by

$$P_l - P_o = 2\sigma_l \cdot \cos(\pi - \alpha)/r \tag{1}$$

where P_l is the pressure of the liquid fuel, P_o is the ambient pressure, σ_l is the surface tension of the liquid fuel, α is the angle between the meniscus and the capillary wall, and r is the radius of the capillary.

The transmeniscus pressure that can be withstood without leakage is limited by the size of the capillary as well as the

surface properties that are associated with the hydrophobic material. Given a surface material and the maximum contact angle (or advancing contact angle θ_a) of the liquid on it, the maximum transmeniscus pressure that is sustainable in this venting capillary, i.e., the leakage onset pressure, is

$$P_{\max} = \mathrm{Max}(P_l) - P_o = 2\sigma_l \cdot \cos(\pi - \theta_a)/r. \qquad (2)$$

If the transmeniscus pressure $(P_l - P_o)$ is higher than this leakage onset pressure, leakage will occur. Here, we have assumed that the venting capillary is straight and the surface of its wall is smooth.

This venting mechanism has been verified by the removal of chemically induced CO_2 bubbles from an inorganic aqueous solution using Teflon-coated silicon-microfabricated venting capillaries [10], [11]. However, leakage of the liquid was observed frequently during the experiments due to the low leakage onset pressure (less than 3 kPa theoretically) [11]. This poor pressure tolerance has been attributed to the relatively large (25 μm in radius) venting capillaries and the poor uniformity of the hydrophobic coatings inside the capillaries.

Leakage prevention is more challenging in μDMFC than in typical water-based microfluidic devices because both the surface tension and the contact angle of the methanol-containing fuel are lower than those of water (Table I). The leakage onset pressure would significantly decrease with increased methanol concentration. Since it is difficult to directly measure the contact angles and surface tensions on the inner surfaces of the venting capillaries, the contact angles were measured on a Teflon-coated flat surface instead to provide a reference. A goniometer (First Ten Ångstroms, Portsmouth, VA) was used to obtain the contact angles with measurement accuracy within 1°. The value from a flat surface provides a reasonable approximation in the absence of direct measurement and can be used to determine the pore size [17], [18].

Due to its higher energy density, a concentrated fuel is usually desired to obtain longer operation time for the microfuel cell. Currently, the fuel concentrations are limited to 0.5–2-M methanol due to the severe crossover of more concentrated fuel. However, progress in PEM technology is expected to alleviate the fuel crossover problem and accommodate higher fuel concentration, up to 10 M [19]. The leakage prevention performance must be greatly improved to make the gas-venting capillaries suitable for μDMFC, considering the trend toward the use of concentrated fuel. While smaller silicon-micromachined venting capillaries and improved hydrophobic coatings are possible, the corresponding lithography-based fabrication techniques would become exceedingly complex and prohibitively costly for eventual commercialization. Challenged by the high methanol concentration and the demanding nanoscale venting capillary fabrication, we identified intrinsically hydrophobic nanoporous membranes for our purpose of gas bubble removal from the concentrated methanol fuel of μDMFCs. This family of membranes has originally been developed for sample preparation of X-ray spectrochemistry, as well as HPLC and ultrafiltration [20], [21]. A broad choice of membranes with diverse material, pore size, and porosity, and relatively low prices are available. The typical size of the pores (with a radius in the range of 0.05–2.5 μm) is ideal for the gas-venting applications.

The nanopores in the membrane can no longer be assumed to be smooth and uniform. Since the surface topology of their inner wall affects the contact angle and even the effective radius, these nanopores are described by a new model that incorporates irregular capillaries, as illustrated in Fig. 2(b), where the leakage onset pressure is defined as

$$P'_{\max} = 2\sigma_l \cdot \mathrm{Max}\left(\cos(\pi - \theta_{a,\mathrm{eff}})/r_{\mathrm{eff}}\right) \qquad (3)$$

with r_{eff} and $\theta_{a,\mathrm{eff}}$ representing the effective radius of venting capillaries and the effective advancing contact angle inside the venting capillaries, respectively. The Max function implies that the leakage onset of each venting capillary is defined by its most constricted *neck*, as shown in Fig. 2(b). In addition, given a membrane that is composed of many capillaries, the leakage onset over an area of the membrane is determined by the most susceptible capillaries. So, the overall leakage onset pressure of the membrane is

$$P_{\mathrm{leak}} = \mathrm{Min}\left(P'_{\max}\right) = \mathrm{Min}\left(2\sigma_l \cdot \mathrm{Max}\left(\frac{\cos(\pi - \theta_{a,\mathrm{eff}})}{r_{\mathrm{eff}}}\right)\right). \qquad (4)$$

III. Membrane Characterization

Two kinds of membranes are employed in this paper: 1) a porous polytetrafluoroethylene (PTFE) membrane (from Millipore) with a nominal pore radius of 1.5 μm [20] and 2) a porous polypropylene membrane (from Chemplex) with a nominal pore radius of 0.1 μm [21].

The leakage onset pressure of hydrophobic nanoporous membranes is measured by using a nitrogen gas tank as the pressure source. The pressure is controlled by a gas regulator and read from a pressure gauge. A liquid reservoir is pressurized to fill the membrane holder containing the porous hydrophobic membrane to be tested. The outlet of the filter holder is connected to a gas flow meter from Cole Parmer, which can detect gas flows of as small as 0.01 mL/min. If the liquid pressure is below the leakage onset pressure, no gas flow will be detected by the gas flow meter. The pressure is gradually increased until a steady flow is measured. This pressure is recorded as the leakage onset pressure. The sensitivity of the gas flow meter aids in more precisely identifying the leakage onset pressure. The gas flow meter is then removed. The liquid mass flux is determined by weighing the effluent liquid and recording the amount of time required.

Both the porous PTFE and porous polypropylene membranes were tested with deionized water and 10-M methanol as the working fluids (Fig. 3). For the porous polypropylene membrane, no leakage was observed until the pressure exceeded 200 kPa (30 $\mathrm{lbf/in^2}$), which indicates that its leakage onset pressure is larger than 200 kPa for both water and 10-M methanol. The pressure was not further increased because the porous polypropylene membrane was found to break at a pressure that is slightly above this value in an earlier paper [22]. A leakage onset pressure of more than 200 kPa can be considered safe for μDMFC, where the working pressure inside

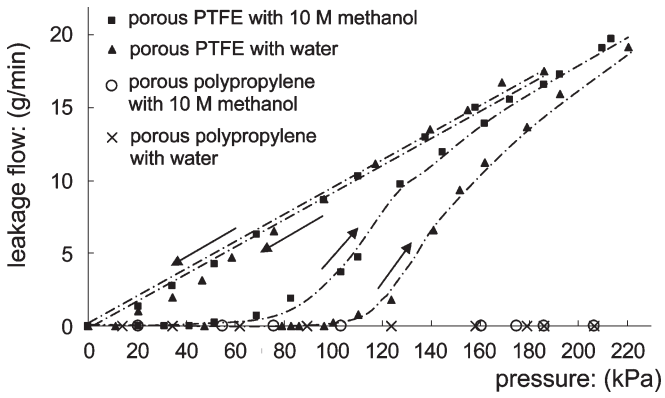

Fig. 3. Flow–pressure curve of hydrophobic nanoporous membranes for water and 10-M methanol.

the fuel stack rarely exceeds 1 $\mathrm{lbf/in^2}$ (6.9 kPa) during normal operation. Therefore, the porous polypropylene membrane can provide reliable leakage prevention for this application. In order to further investigate the liquid penetration phenomena and verify the liquid-holding mechanism, the same test has also been conducted with a piece of porous PTFE membrane, for which we were able to observe the leakage. The result showed leakage onset pressures of ∼41 kPa for 10-M methanol and ∼96 kPa for water, after which the leakage flow increased with the pressure. The pressure was increased up to ∼200 kPa and then decreased. A linear relationship between the pressure and the leakage flow was found when the pressure was decreased, following Darcy's law. These asymmetric data indicate that the leakage is directional and further confirm the liquid-holding mechanism of hydrophobic venting membranes described in Fig. 2. This type of flow–pressure curve is typical for hydrophobic filter membranes [17] and is often used to determine pore size [18].

The theoretical and experimental values of leakage onset pressure are summarized in Table II. Since r_{eff} and $\theta_{a,\mathrm{eff}}$ are difficult to measure, (4) cannot be directly applied. The theoretical value is hence calculated from (2), using the properties in Table I and the nominal radii specified by the manufacturers. The measured data show that the calculated values of the leakage onset pressure are conservative. The higher-than-expected leakage onset pressure is attributed to the irregular shape of the capillaries, which are schematically illustrated in Fig. 2(b) and supported by the scanning electron microscope (SEM) pictures of the porous membrane in Fig. 4.

Due to the strict requirement of leakage prevention in μDMFCs, the porous polypropylene membrane is considered as the proper choice for this application. The investigations hereafter are focused on the devices constructed with the porous polypropylene membrane.

IV. Device Fabrication and Testing

The components of a gas-venting microchannel test unit and their assembly process are illustrated in Fig. 5. The microchannel chip and membrane holder chip were both fabricated from a 400-μm-thick (100) silicon wafer by deep reactive ion etching (DRIE). A cross-shaped gas bubble generator [23] was also designed on the microchannel chip to produce a liquid/gas two-phase flow, corresponding to a μDMFC's fuel flow with CO_2 bubbles. Parts of the microchannel on the chip were protected by polyimide tape after the first DRIE had reached the desired depth. After DRIE and subsequent Piranha cleaning, the microchannel chip was anodically bonded to a piece of Pyrex glass. The membrane was then sandwiched between the microchannel chip and the membrane holder chip with epoxy to complete a gas-venting microchannel, imitating the anodic microchannel of a μDMFC. During the epoxy adhesive bonding, through-holes on both chips were used as alignment marks. The alignment was assisted by strong illumination from below, which can penetrate the semitransparent porous membrane [Fig. 5(a)].

The finished test unit, as shown in Fig. 5(b) and (c), was then incorporated into the test apparatus illustrated in Fig. 6. A nitrogen gas tank was used to provide a gas flow into the test unit. Another nitrogen gas tank was used to provide a liquid flow via a liquid reservoir. The two flows were mixed on the chip to form the two-phase flow, which is introduced into the downstream gas-venting microchannels. The gas bubbles in the two-phase flow were removed, eventually leaving single-phase liquid in the microchannel. The experimental conditions were monitored by a pressure sensor and a gas flow meter and controlled by pressure regulators and valves.

Both water and 10-M methanol were tested to verify the bubble removal function of the gas-venting microchannel. The transmembrane pressure $(P_l - P_o)$ was controlled to within the range of 3.4–13.8 kPa (0.5–2.0 $\mathrm{lbf/in^2}$). Reliable venting has been observed in all the tests. Fig. 7 shows a typical bubble venting process for a gas-venting microchannel under a transmembrane pressure of 6.9 kPa (1 $\mathrm{lbf/in^2}$). In this particular test, a piece of porous polypropylene membrane is employed, and 10-M methanol is used as the working fluid. The essentially same venting behavior has also been observed in gas-venting microchannels that are constructed with porous PTFE.

V. Venting Threshold

Although bubble removal through gas venting is confirmed for both water and 10-M methanol, the two-phase flows in a gas-venting microchannel behave differently for the two cases. In water, once the leading gas bubble reaches the uncovered porous membrane, it begins to be vented, as demonstrated in Fig. 8(a). However, in the 10-M methanol solution, bubbles travel some distance in the form of a bubble train and coalesce into a leading bubble at the downstream, where venting finally starts. This bubble train can be relatively long before venting is accomplished, as shown in Fig. 8(b). We term this phenomenon of delayed venting as the "venting threshold" because the experiments suggest that the bubbles need to overcome a certain obstacle before they can be removed.

We conjecture two possible explanations to describe the venting threshold. As illustrated in Fig. 9(a), one hypothesis assumes that a thin liquid film forms between the bubble and the venting capillary, blocking the entrance to the capillary. A certain amount of time is required for the thin liquid film to

TABLE II
LEAKAGE ONSET PRESSURE: CALCULATED AND MEASURED VALUES

	Porous PTFE			Porous polypropylene		
	nominal radius	calculated value (kPa)	measured value (kPa)	nominal radius	calculated value (kPa)	measured value (kPa)
10 M methanol	1.5 μm	10	~ 41	0.1 μm	150	> 200
DI water		51	~ 96		760	> 200

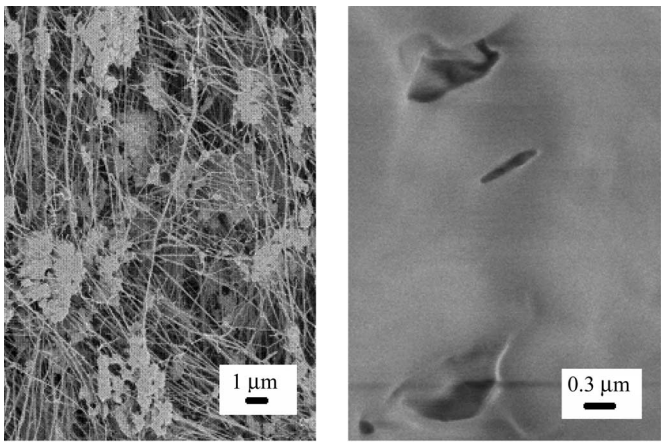

Fig. 4. SEM pictures of the porous membranes' surface. (a) Porous PTFE. (b) Porous polypropylene.

break; then, the gas bubble can be easily vented out. Fig. 9(b) shows an alternative hypothesis in which gas venting is blocked by the presence of a tiny liquid droplet trapped within the venting capillary. The droplet can withstand a certain pressure, depending on the resistance created by contact angle hysteresis. These tiny droplets, although deep in a long capillary, are subject to evaporation due to their large area-to-volume ratios, which can explain the eventual clearance of the venting capillaries.

Both of the hypotheses can be supported by two observations: First, experiments with water demonstrate little or no venting threshold. In the liquid film hypothesis of Fig. 8(a), this can be explained by the larger contact angle of water, which significantly increases the dewetting velocity of the holes in the liquid film [24]. In the droplet hypothesis of Fig. 9(b), this can be explained by the small contact angle hysteresis of water (Table I), which renders the trapped water droplets much easier to be removed. Second, the bubble train is observed to be much shorter when the flow rate is reduced by decreasing the transmembrane pressure, as shown in Fig. 8(c). This can be explained by the fact that a certain time is required to break the liquid film or clear the capillary. When the flow is slower, the venting threshold is removed after a bubble travels a shorter distance. The preceding hypotheses are supported by our observations. Considering that the pores are in nanometer scale, other hypotheses (e.g., the introduction of very high pressure or even clathrate formation) should not be excluded for further investigations. The mechanism of venting threshold is worthy of further investigations, which could lead to minimal venting threshold and quicker venting rate.

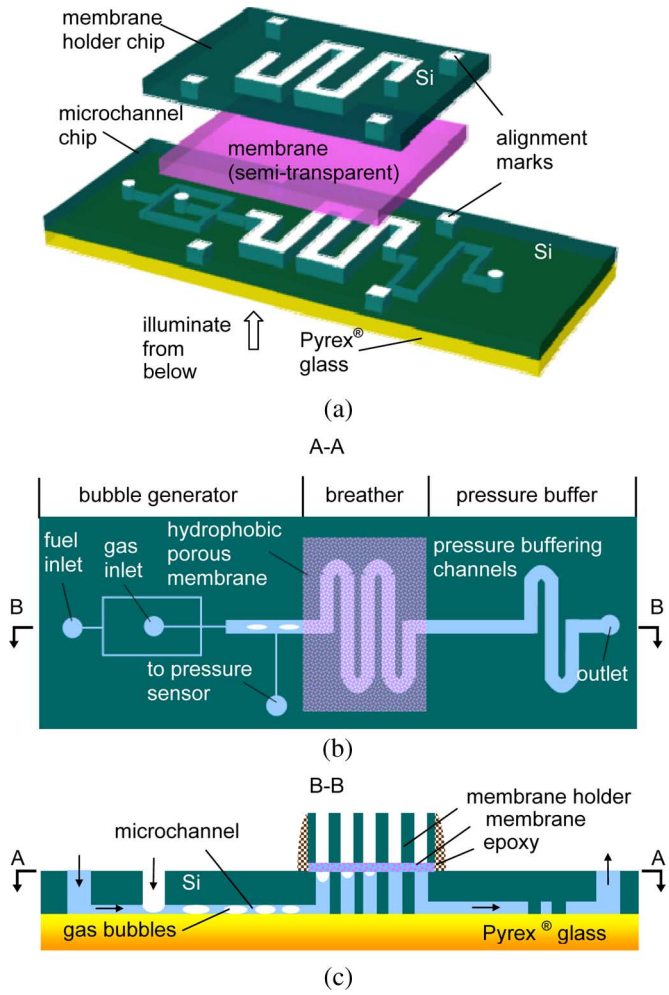

Fig. 5. Gas-venting microchannel with on-chip bubble injector. (a) Perspective view during alignment and bonding. (b) Horizontal cross section (A–A view) of a completed device. (c) Vertical cross section (B–B view) of a completed device.

VI. VENTING RATE

An ideal gas-venting microchannel should be able to both tolerate high inner pressure and quickly remove gas. With a satisfactory leakage onset pressure, the venting rate of the microchannel is investigated. The venting rate quantifies how rapidly the gas bubbles can be removed. The gas flow rate through porous membranes can be modeled using Darcy's law. Analogous to electrical resistance, the transmembrane fluidic resistance is defined as the proportion of the transmembrane pressure $(P_b - P_o)$ to the transmembrane gas flow rate Q_g (venting rate), where P_b is the pressure inside the bubble. Assuming a uniform distribution of pores on the membrane with a pore density of n, the total number of pores on an

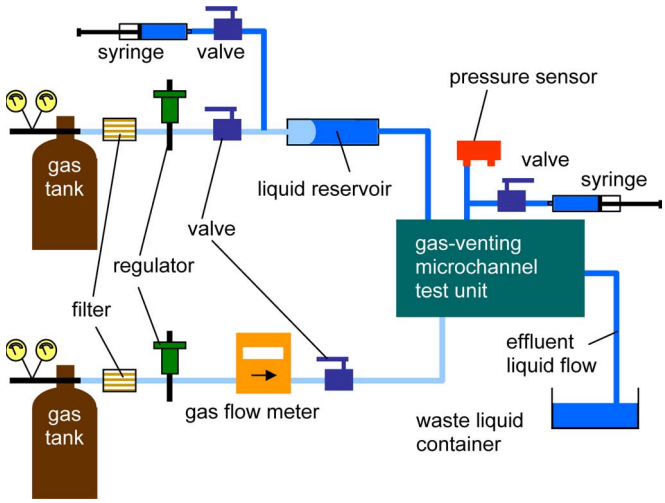

Fig. 6. Experimental apparatus to test the gas-venting microchannels made with porous hydrophobic membranes.

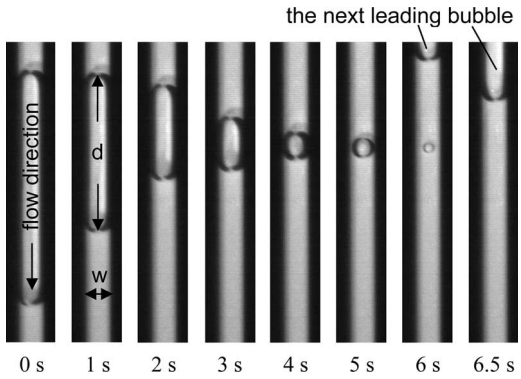

Fig. 7. Exemplary venting process in a gas-venting microchannel. The video clips were taken from a two-phase flow of 10-M methanol and nitrogen gas bubbles along a microchannel made with porous polypropylene membrane. The device is horizontally positioned with respect to gravity.

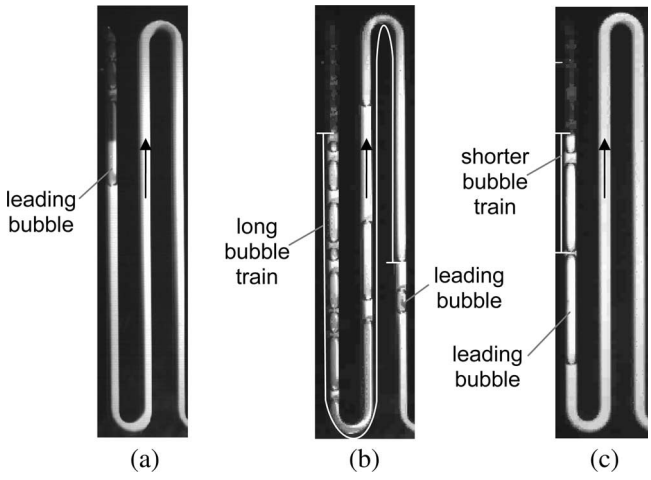

Fig. 8. Venting threshold. (a) Water: $P_l - P_o = 5.5$ kPa. (b) 10-M methanol: $P_l - P_o = 5.5$ kPa. (c) 10-M methanol: $P_l - P_o = 3.4$ kPa.

area of A is $N = nA$. If the average flow resistance of a pore is R_i, the flow resistance for a venting area A is written as $R_A = R_i/nA$, with R_i and n being intrinsic constants of a given membrane. Assuming that the whole microchannel cross

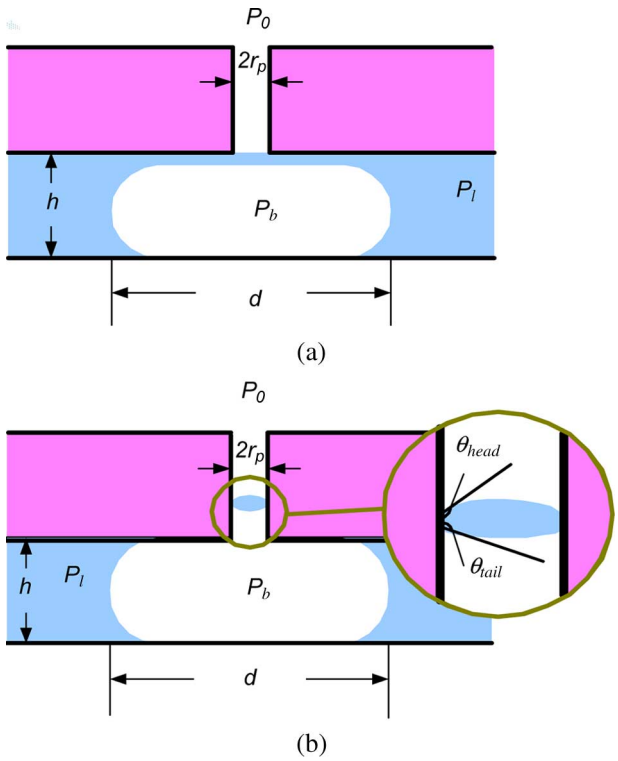

Fig. 9. Hypothetical explanations for the venting threshold: (a) by a thin liquid film and (b) by a trapped droplet.

section is occupied by a gas bubble, venting rate Q_g can be related to a bubble shrinking rate $\partial d/\partial t$, i.e.,

$$Q_g \approx w \cdot h \cdot \partial d/\partial t \tag{5}$$

where w, h, and d are the channel width, channel depth, and bubble length, respectively, as shown in Fig. 7. In our experiments, the channel depth and width are always kept the same $(h = w)$ to maintain a square cross section and simplify the analysis. Therefore, the transmembrane pressure can be related to the bubble shrinking rate as follows:

$$P_b - P_o = -R_A \cdot Q_g = -\frac{R_i}{n \cdot kwd} w^2 \frac{\partial d}{\partial t} \tag{6}$$

where k is a geometric constant that takes into account the fact that the bubble does not occupy the entire microchannel cross section. Indeed, the corners of the square microchannel can be filled with water, and a liquid thin film may exist between the bubble and the membrane. According to (6), bubble length d is the solution of a first-degree differential equation given by

$$d = -\frac{R_i w}{kn(P_b - P_o)} \cdot \frac{\partial d}{\partial t} = -\frac{1}{K(P_b - P_o)} \cdot \frac{\partial d}{\partial t} \tag{7}$$

where $K = nk/(R_i w)$ is determined by fuel concentration as well as the geometry and material of the microchannel. During the venting process of an elongated bubble, K can be assumed to be a constant. We choose $t = 0$ as the moment the bubble length d reaches the channel width w. The boundary condition can be applied as $t = 0$ and $\ln(d/w) = 0$. The transmembrane pressure $(P_l - P_o)$ is measured and used to approximate

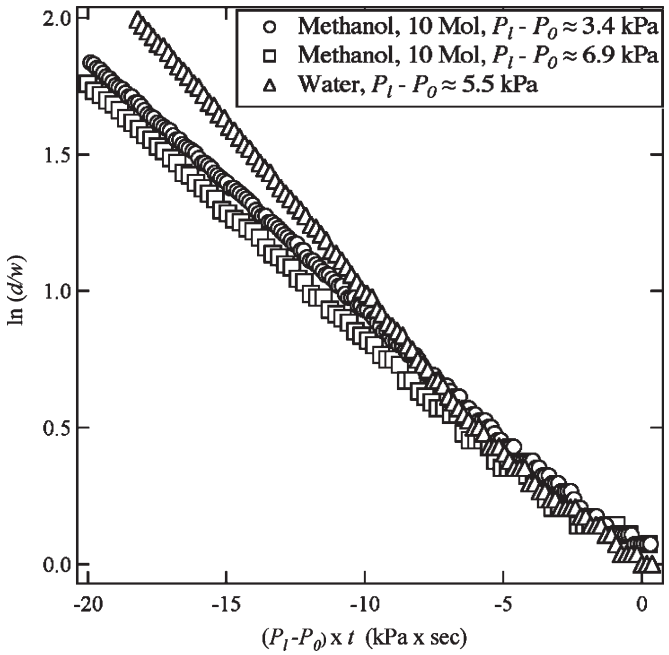

Fig. 10. Evolution of elongated bubble length d as a function of time and transmembrane pressure (experimental data obtained in a gas-venting microchannel constructed by the porous polypropylene membrane).

$(P_b - P_o)$, which is difficult to measure directly. In the experiments, the transmembrane pressure $(P_l - P_o)$ is kept between 3.4 kPa (0.5 lbf/in^2) and 6.9 kPa (1 lbf/in^2) and is much larger than the capillary pressure of the bubble, which is estimated as $P_b - P_l = 4\sigma_l/w$ ($\sim$0.7 kPa), so as to provide meaningful approximation. Overall, the length of the elongated bubble can be expressed as a function of time, i.e.,

$$\ln(d/w) = -K(P_b - P_o)\cdot t \approx -K(P_l - P_o)\cdot t, \qquad (t<0). \tag{8}$$

After the bubble shrinks to the dimension of channel width w (i.e., $t > 0$), (8) can no longer be applied because the capillary pressure becomes significant. With a significantly increased inner pressure P_b, the smaller bubbles are removed much faster than (8) predicts. However, the venting rate of elongated bubbles is more relevant because they cause the most severe bubble clogging problems.

The experimental video is analyzed by an image process software (ImageJ [25]) to verify (8). The evolution of elongated bubble length d is measured over time. Fig. 10 shows that the experimental results agree with the behavior expected from (8) for both water and 10-M methanol solution. The measured venting rate coefficient $K_{\mathrm{EXP}}(\sim 0.1(\mathrm{kPa}\times \mathrm{s})^{-1})$ is much smaller than the measurement in the absence of liquid (i.e., $k = 1$): $K_0(\sim 0.6(\mathrm{kPa}\times \mathrm{s})^{-1})$. In other words, the venting is slower when the microchannel is filled with liquid. Several factors contribute to this effect. In particular, the venting rate is directly related to the available dry surface on the membrane. Since the membrane surface is wetted before a bubble arrives, a considerable number of pores can be prevented from venting by a thin liquid film or tiny droplets in the pores, as explained in the previous section. The venting rate is therefore limited by dewetting velocity $U(\theta)$, which depends on the contact angle [24]. In addition, the liquid fuel pressure P_l was measured at the inlet of the gas-venting microchannel. The exact fuel pressure surrounding a venting bubble is smaller and varies with the venting location.

Since only the longitudinal bubble reduction is considered, the preceding analysis describes a 1-D venting model. Further investigations will consider the venting rate of a bubble squeezed between two plates (2-D venting) and an unconfined bubble on a porous membrane (3-D venting).

VII. Conclusion

In order to solve the bubble-clogging problem of microfluidic devices, particularly, microfuel cells such as μDMFC, hydrophobic venting has been developed to directly remove gas bubbles from methanol aqueous solutions in the anodic microchannel. Commercially available hydrophobic nanoporous membranes have been explored to design the functionality of gas venting for μDMFC by taking advantage of the well-established membrane technologies. Porous PTFE and porous polypropylene were employed to construct gas-venting microchannels, which are able to remove gas bubbles from both water and 10-M methanol aqueous solution. Under our experimental condition, the porous polypropylene membrane was proven to provide leakage prevention for even 10-M methanol with a leakage onset pressure of more than 200 kPa, which can be considered safe for the normal operation of μDMFC. The removal of gas bubbles was experimentally verified and characterized, paving the way for its application in μDMFCs. The gas-venting microchannel can be integrated into existing μDMFC systems to alleviate the high flow resistance caused by bubbles, release pressure buildup, avoid methanol crossover, and reduce the danger of fuel/catalyst/electrode isolation. A 1-D model describing the venting rate has been developed and experimentally verified to provide a guideline for future designs. Further investigations into the venting rate and venting threshold are expected to elucidate some fundamental issues on the behaviors of microscopic bubbles and droplets inside microchannels and nanopores.

Acknowledgment

The authors would like to thank Prof. C. Y. Wang, Prof. X. Zhang, Prof. X. Zhong, B. V. Dyk, Dr. T. J. Yen, Dr. G. Q. Lu, and Dr. M. Tatineni for the discussion and help.

References

[1] P. Gravesen, J. Branebjerg, and O. S. Jensen, "Microfluidics—A review," *J. Micromech. Microeng.*, vol. 3, no. 4, pp. 168–182, Dec. 1993.

[2] T. Cubaud and C.-M. Ho, "Transport of bubbles in square microchannels," *Phys. Fluids*, vol. 16, no. 12, pp. 4575–4585, Dec. 2004.

[3] J. Kohnle, G. Waibel, R. Cernosa, M. Storz, H. Ernst, H. Sandmaier, T. Strobelt, and R. Zengerle, "A unique solution for preventing clogging of flow channels by gas bubbles," in *Proc. 15th IEEE Int. Conf. Micro Electro Mech. Syst.*, Las Vegas, NV, Jan. 2002, pp. 77–80.

[4] M. J. Jensen, "Bubbles in microchannels," M.S. thesis, Tech. Univ. Denmark, Copenhagen, Denmark, 2002.

[5] C. Litterst, S. Eccarius, C. Hebling, R. Zengerle, and P. Koltay, "Novel structure for passive CO_2 degassing in μDMFC," in *Proc. 19th IEEE Int. Conf. Micro Electro Mech. Syst.*, Istanbul, Turkey, 2006, pp. 102–105.

[6] E. Sakaue, "Micromachining/nanotechnology in direct methanol fuel cell," in *Proc. 18th IEEE Int. Conf. Micro Electro Mech. Syst.*, Miami, FL, 2005, pp. 600–605.
[7] G. Q. Lu and C. Y. Wang, "Electrochemical and flow characterization of a direct methanol fuel cell," *J. Power Sources*, vol. 134, no. 1, pp. 33–40, Jul. 2004.
[8] C. W. Wong, T. S. Zhao, Q. Ye, and J. G. Liu, "Transient capillary blocking in the flow field of a micro-DMFC and its effect on cell performance," *J. Electrochem. Soc.*, vol. 152, no. 8, pp. A1600–A1605, 2005.
[9] M. Hogarth, "Chapter 7: Prospects of the direct methanol fuel cell," in *Fuel Cell Technology Handbook*. Boca Raton, FL: CRC Press, 2003.
[10] D. D. Meng, J. Kim, and C.-J. Kim, "A distributed gas breather for micro direct methanol fuel cell (μDMFC)," in *Proc. 16th IEEE Int. Conf. Micro Electro Mech. Syst.*, Kyoto, Japan, Jan. 2003, pp. 534–537.
[11] D. D. Meng, J. Kim, and C.-J. Kim, "A degassing plate with hydrophobic bubble capture and distributed venting for microfluidic devices," *J. Micromech. Microeng.*, vol. 16, no. 2, pp. 419–424, Feb. 2006.
[12] M. Chiao, K. B. Lam, and L. Lin, "Micromachined microbial fuel cells," in *Proc. 16th IEEE Int. Conf. Micro Electro Mech. Syst.*, Kyoto, Japan, Jan. 2003, pp. 383–386.
[13] Z. Yang, S. Matsumoto, and R. Maeda, "A prototype of ultrasonic microdegassing device for portable dialysis system," *Sens. Actuators A, Phys.*, vol. 95, no. 2/3, pp. 274–280, Jan. 2002.
[14] K. D. Pickering, L. Y. Hammond, and J. L. Garland, "Immobilized microbe microgravity water processing system (IMMWPS) flight experiment," presented at the Bioastronautics Investigators' Workshop, Galveston, TX, Jan. 2001, Paper 116.
[15] A. Weston and P. Brown, *HPLC and CE: Principles and Practice*. San Diego, CA: Academic, 1997.
[16] A. Guenther, M. Jhunjhunwala, M. A. Schmidt, and K. F. Jensen, "Liquid mixing using inert gas and an integrated gas-liquid separator," in *Proc. Int. Conf. μTAS*, Squaw Valley, CA, Oct. 2003, pp. 465–468.
[17] M. C. Garcia-Payo, M. A. Izquierdo-Gil, and C. Fernandez-Pineda, "Wetting study of hydrophobic membranes via liquid entry pressure measurements with aqueous alcohol solutions," *J. Colloid Interface Sci.*, vol. 230, no. 2, pp. 420–431, Oct. 2000.
[18] K. S. McGuire, K. W. Lawson, and D. R. Lloyd, "Pore size distribution determination from liquid permeation through microporous membranes," *J. Membr. Sci.*, vol. 99, no. 2, pp. 127–137, Feb. 1995.
[19] T. Yamaguchi, Y. Nishiyama, A. Yamauchi, and H. Zhou, "Novel design methodology for fuel cell MEAs using a nano-scale modeling," in *Proc. 2nd Int. Conf. Polymer Batteries Fuel Cells*, Las Vegas, NV, Jun. 2005. abstract 187.
[20] *Fluoropore Membrane Filters*. [Online]. Available: http://www.millipore.com/catalogue.nsf/docs/C254
[21] *Chemplex's X-Ray Spectrochemical Sample Preparation*. [Online]. Available: http://www.chemplex.com/
[22] D. S. Meng, T. Cubaud, C.-M. Ho, and C.-J. Kim, "A membrane breather for micro fuel cells with high concentration methanol," in *Proc. Tech. Dig. Solid-State Sens., Actuators, Microsyst. Workshop*, Hilton Head Island, SC, Jun. 2004, pp. 141–144.
[23] T. Cubaud, M. Tatineni, X. Zhong, and C.-M. Ho, "Bubble dispenser in microfluidic devices," *Phys. Rev. E, Stat. Phys. Plasmas Fluids Relat. Interdiscip. Top.*, vol. 72, no. 3, p. 037302, Sep. 2005.
[24] C. Reudon, F. Brochard-Wyart, and F. Rondelez, "Dynamics of dewetting," *Phys. Rev. Lett.*, vol. 66, no. 6, pp. 715–718, Feb. 1991.
[25] *ImageJ: Image Processing and Analysis in Java*. [Online]. Available: http://rsb.info.nih.gov/ij/

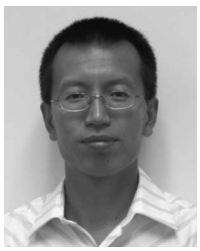

Dennis Desheng Meng (M'05) received the Ph.D. degree in mechanical engineering from the University of California, Los Angeles (UCLA), in 2005.

He is currently an Assistant Professor with the Department of Mechanical Engineering–Engineering Mechanics, Michigan Technological University, Houghton. He is directing the Multi-Scale Energy System (MuSES) Laboratory with primary research interests in scalable micro- and nanotechnologies for energy and environmental applications. His research has been focused on the microfluidic aspect of microdirect methanol fuel cells, particularly, nanoporous hydrophobic venting to remove the CO_2 gas byproduct and an embedded self-pumping mechanism to circulate the liquid fuel with an ultracompact configuration.

Dr. Meng was the recipient of the 2006 UCLA Outstanding Ph.D. Award in Mechanical Engineering.

Thomas Cubaud received the Ph.D. degree from Paris-Sud University, Paris, France, and The City of Paris Industrial Physics and Chemistry Higher Educational Institution (ESPCI), Paris, in 2001.

He was a Postdoctoral Research Scientist with the Department of Mechanical and Aerospace Engineering, University of California, Los Angeles (UCLA), where he worked on the motion of gas bubbles in microchannels to optimize the performance of microdirect methanol fuel cells. He was also with the Department of Chemistry and Biochemistry, UCLA, where he worked on microscale physicochemical hydrodynamic instabilities. He is currently an Assistant Professor with the Department of Mechanical Engineering, Stony Brook University, Stony Brook, NY.

Dr. Cubaud was the recipient of the 2005 and 2006 Annual Gallery of Fluid Motion Awards from the American Physical Society and the 2006 UCLA Chancellor's Award for Postdoctoral Research.

Chih-Ming Ho (M'00) received the Ph.D. degree from The Johns Hopkins University, Baltimore, MD.

He is the Ben Rich-Lockheed Martin Chair Professor in the School of Engineering, University of California, Los Angeles (UCLA). He is the Director of the Institute for Cell Mimetic Space Exploration (http://www.cmise.org) and the Director of the Center for Cell Control (http://CenterForCellControl.org). He served as UCLA Associate Vice Chancellor for Research from 2001 to 2005. He is known for his work in micro/nano fluidics, bio-nano technologies, and turbulence. He has published 260 papers and presented over 130 keynote talks at international conferences and 15 named distinguished talks.

Dr. Ho was ranked by ISI as one of the top 250 most cited researchers worldwide in the entire engineering category. In 1997, he was inducted as a member of the National Academy of Engineering. In 1998, he was elected as an Academician of Academia Sinica. He is the holder of five honorary professorships. He was elected as a Fellow of the American Physical Society as well as the American Institute of Aeronautics and Astronautics for his contributions in a wide spectrum of technical areas.

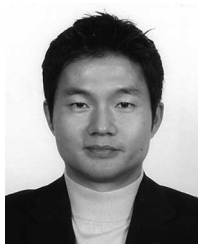

Chang-Jin (CJ) Kim (M'88) received the B.S. degree from Seoul National University, Seoul, Korea, in 1981, the M.S. degree from Iowa State University, Ames, in 1985, and the Ph.D. degree in mechanical engineering from the University of California, Berkeley, in 1991.

Since joining the faculty at the University of California, Los Angeles (UCLA), in 1993, he has developed several microelectromechanical systems (MEMS) courses and established a MEMS Ph.D. major field in the Department of Mechanical and Aerospace Engineering. Directing the Micro and Nano Manufacturing Laboratory, he is also an IRG Leader for the NASA-supported Institute for Cell Mimetic Space Exploration, UCLA, and a founding member of the California NanoSystems Institute, UCLA. His research interests are MEMS and nanotechnology, including the design and fabrication of micro/nanostructures, actuators, and systems, with a focus on the use of surface tension.

Dr. Kim has served on numerous Technical Program Committees, including Transducers and the IEEE MEMS Conference, and on the US Army Science Board as a Consultant. He is currently chairing the Devices and Systems Committee of the ASME Nanotechnology Institute and serving as a Subject Editor for the IEEE/ASME *Journal of Microelectromechanical Systems*. He is also serving on the Editorial Advisory Board of the *IEEJ Transactions on Electrical and Electronic Engineering* and on the National Academies Panel on Benchmarking the Research Competitiveness of the U.S. in Mechanical Engineering. He was the recipient of the Graduate Research Excellence Award from Iowa State University, the 1995 TRW Outstanding Young Teacher Award, the 1997 National Science Foundation CAREER Award, and the 2002 ALA Achievement Award.